

## The effect of alkali niobate addition on the phase stability and dielectric properties of $\text{Pb}(\text{Zn } 1/3 \text{ Nb } 2/3) \text{O}_3$ based ceramic

Jong-Sung Park, Jung-Kun Lee, and Kug Sun Hong

Citation: *Journal of Applied Physics* **101**, 114101 (2007); doi: 10.1063/1.2733612

View online: <http://dx.doi.org/10.1063/1.2733612>

View Table of Contents: <http://scitation.aip.org/content/aip/journal/jap/101/11?ver=pdfcov>

Published by the AIP Publishing

### Articles you may be interested in

Dielectric and AC-conductivity studies of  $\text{Dy}_2\text{O}_3$  doped  $(\text{K}_{0.5}\text{Na}_{0.5})\text{NbO}_3$  ceramics

*AIP Advances* **4**, 087113 (2014); 10.1063/1.4892856

Enhanced dielectric, ferroelectric, and electrostrictive properties of  $\text{Pb}(\text{Mg}_{1/3}\text{Nb}_{2/3})_{0.9}\text{Ti}_{0.1}\text{O}_3$  ceramics by  $\text{ZnO}$  modification

*J. Appl. Phys.* **113**, 204101 (2013); 10.1063/1.4801881

Structural change in polar nanoregion in alkali niobate added  $\text{Pb}(\text{Zn}_{1/3}\text{Nb}_{2/3})_{0.95}\text{Ti}_{0.05}\text{O}_3$  single crystal and its effect on ferroelectric properties

*J. Appl. Phys.* **112**, 074109 (2012); 10.1063/1.4757620

$(1-x)\text{BaTiO}_3-x(\text{Na}_{0.5}\text{K}_{0.5})\text{NbO}_3$  ceramics for multilayer ceramic capacitors

*Appl. Phys. Lett.* **90**, 132905 (2007); 10.1063/1.2717559

Relaxorlike dielectric properties and history-dependent effects in the lead-free  $\text{K}_{0.5}\text{Na}_{0.5}\text{NbO}_3-\text{SrTiO}_3$  ceramic system

*Appl. Phys. Lett.* **85**, 994 (2004); 10.1063/1.1779947

## 2014 Special Topics



PEROVSKITES



2D MATERIALS



MESOPOROUS MATERIALS



BIOMATERIALS/  
BIOELECTRONICS



METAL-ORGANIC  
FRAMEWORK  
MATERIALS



Submit Today!

# The effect of alkali niobate addition on the phase stability and dielectric properties of $\text{Pb}(\text{Zn}_{1/3}\text{Nb}_{2/3})\text{O}_3$ based ceramic

Jong-Sung Park

*School of Materials Science and Engineering, Seoul National University, Seoul 151-744, Korea*

Jung-Kun Lee

*Materials Science and Technology Division, Los Alamos National Laboratory, Los Alamos, New Mexico 87545*

Kug Sun Hong<sup>a)</sup>

*School of Materials Science and Engineering, Seoul National University, Seoul 151-744, Korea*

(Received 26 August 2006; accepted 18 March 2007; published online 1 June 2007)

While  $\text{Pb}(\text{Zn}_{1/3}\text{Nb}_{2/3})\text{O}_3$ – $\text{PbTiO}_3$  (PZN-PT) single crystals have shown superior ferroelectric properties, less scientific and technical interests have been placed on PZN-PT polycrystalline ceramics due to their poor thermodynamic stability and the difficult processing conditions. Here, we stabilized the PZN-PT based ceramics by adding alkali niobates such as  $\text{NaNbO}_3$  (NN) and  $\text{KNbO}_3$  (KN) and investigated their structure and dielectric properties. Two stabilization mechanisms are suggested in alkali niobate added PZN-PT ceramics, increased tolerance factor and enhanced electronegativity difference. KN stabilized the perovskite structure of PZN-PT based ceramics more effectively than NN. Both PZN-PT-KN and PZN-PT-NN ceramics showed the typical behavior of relaxor ferroelectrics. The temperature of maximum dielectric constant of PZN-PT-NN was slightly higher than that of the PZN-PT-KN, which was explained by the difference in ionic size and *B*-site ordering. © 2007 American Institute of Physics. [DOI: [10.1063/1.2733612](https://doi.org/10.1063/1.2733612)]

## I. INTRODUCTION

Relaxor ferroelectric materials with the general formula  $\text{Pb}(\text{B}'\text{B}'')\text{O}_3$  are of great interest because of their high piezoelectric constants and electromechanical coefficients. Among them,  $\text{Pb}(\text{Zn}_{1/3}\text{Nb}_{2/3})\text{O}_3$ – $\text{PbTiO}_3$  (PZN-PT) single crystals have shown excellent piezoelectric properties ( $K_p \sim 92\%$ ,  $d_{33} = 2500$  pC/N) near a morphotropic phase boundary (MPB) between rhombohedral and tetragonal phases.<sup>1</sup> However, since the PZN-PT system has poor thermodynamic stability, it can be synthesized only by adding excess Pb flux at high temperature or applying high pressure. The instability of PZN-PT is attributed to (i) mutual interaction between the lone pairs of the  $\text{Pb}^{2+}$  cation and  $\text{Zn}^{2+}$  cations and (ii) short Pb–O bond length.<sup>2,3</sup> To synthesize the PZN based ceramics, other perovskite materials such as  $\text{BaTiO}_3$  (BT) and  $\text{SrTiO}_3$  (ST) are added as phase stabilizers.<sup>4,5</sup> The stabilization of PZN by partially substituted BT and ST was explained using tolerance factor or electronegativity difference. To make the perovskite structure stable, the former is required to be within proper value of ionic radius for the perovskite structure and the latter is required for strong ionic bond. BT and ST well satisfy these conditions because the tolerance factor of  $\text{BaTiO}_3$  (1.06) and  $\text{SrTiO}_3$  (1.00) compensates the small tolerance factor of PZN (0.986) and the electronegativity difference of  $\text{BaTiO}_3$  (2.23) and  $\text{SrTiO}_3$  (2.20) increases that of PZN (1.80). However, because of the low Curie temperature of BT and ST, the 10 mol % addition of BT decreased the temperature of maximum dielectric constant ( $T_{\max}$ ) of

PZN-PT based ceramics to below about 60 °C and the addition of ST reduced the  $T_{\max}$  of PZN based ceramic more seriously.<sup>6,7</sup> Therefore the dependence of piezoelectric properties on temperature is increased in PZN-PT-BT and PZN-PT-ST based ceramics.

In this study, we stabilize PZN based ceramics by adding alkali niobates and investigate their phase transition behavior and dielectric properties.  $\text{KNbO}_3$  (KN) is ferroelectric with orthorhombic perovskite structure at room temperature and has the same sequence of phase transition as  $\text{BaTiO}_3$  (rhombohedral  $\leftrightarrow$  orthorhombic  $\leftrightarrow$  tetragonal  $\leftrightarrow$  cubic phase) but all the transitions occur at higher temperature than  $\text{BaTiO}_3$ .  $\text{NaNbO}_3$  (NN) is antiferroelectric with orthorhombic perovskite structure at room temperature and is transformed to the cubic structure above 640 °C.<sup>7–9</sup> Therefore, the increased thermal stability of PZN based ceramics is expected in PZN-PT-KN and PZN-PT-NN systems. Alkali ions have been widely used to control the electric properties of perovskite ferroelectrics.<sup>10–12</sup> In both  $\text{Pb}(\text{Zr},\text{Ti})\text{O}_3$  (PZT) and PZN, the alkali ions substituting for A-site ions work as electric hardener. They increase coercive field and quality factor ( $Q_m$ ), and lower dielectric constant and dielectric loss.<sup>10</sup> The effect of the acceptor on the electrical properties has been attributed to the formation of oxygen vacancies to keep charge neutrality in solid solutions. However, in this study, increase in the concentration of oxygen vacancies by adding alkali niobate is negligible because  $\text{Nb}^{5+}$  in *B*-site of the perovskite structure compensates the negative charge of the alkali ions in A-site of the perovskite structure. Therefore, the other factors such as the tolerance factor and the electronegativity difference become more important in this work. Here, we present the structural stability against temperature

<sup>a)</sup>Author to whom correspondence should be addressed; electronic mail: [ksongss@plaza.snu.ac.kr](mailto:ksongss@plaza.snu.ac.kr)

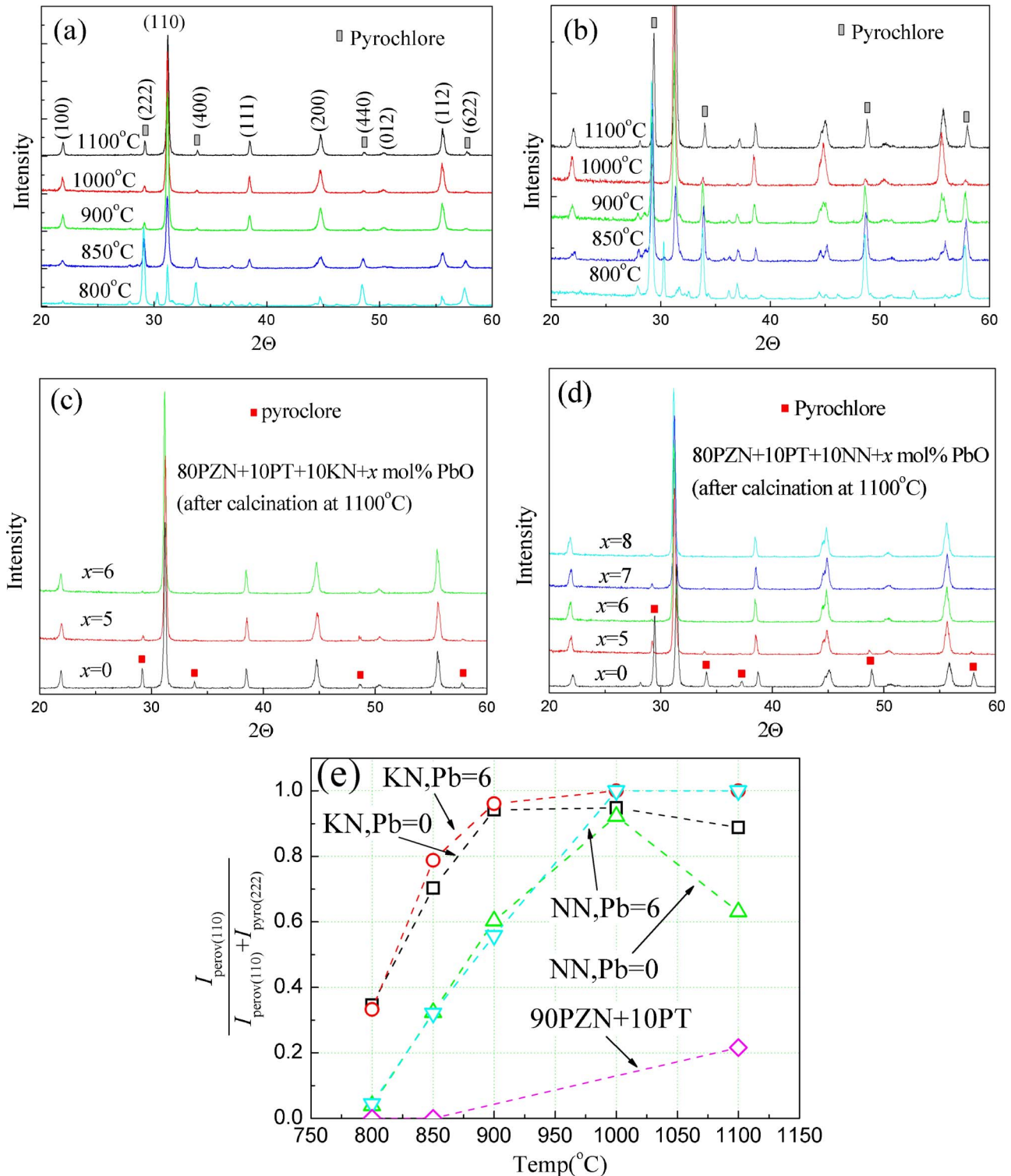


FIG. 1. (Color online) XRD results of 80% PZN+10% PT+10% RN ( $R=\text{K, Na}$ ) after calcinations as a function of temperature and PbO excess; (a) 80PZN+10PT+10KNbO<sub>3</sub>, (b) 80PZN+10PT+10NaNbO<sub>3</sub>, (c) 80PZN-10PT-10KN+x mol% PbO after calcination at 1100 °C, (d) 80PZN-10PT-10KN+x mol% PbO after calcination at 1100 °C, and (e) a ratio of perovskite phase in various PZN-PT-RN.

and the effects of A-site cation on the dielectric properties of alkali niobate doped PZN, and discuss the nature of the phase stability.

## II. EXPERIMENTAL PROCEDURES

The compositions of the PZN-PT-RN ( $R=\text{Na, K}$ ) solid solution were prepared containing various amounts of PT

across the MPB using the mixed oxide method. Reagent-grade PbO, ZnO, Nb<sub>2</sub>O<sub>5</sub>, K<sub>2</sub>CO<sub>3</sub>, Na<sub>2</sub>CO<sub>3</sub>, and TiO<sub>2</sub> powders were used as the starting materials. Starting materials were weighed, and then mixed for 24 h with stabilized ZrO<sub>2</sub> media and ethanol. After drying, the mixed powders were calcined for 2 h at 850 °C. The calcined powders were ball milled for 24 h. The dried powders were granulated, pressed

into pellets with 1000 kg/cm<sup>2</sup> uniaxial pressure, then sintered with PbO atmospheric powders in a covered crucible at 1000–1100 °C for 2 h.

The crystal structure of solid solution samples was investigated using x-ray diffraction. Data collection was performed in the  $2\theta$  range of 20°–60° using a Bragg-Brentano diffractometer and Cu  $K_{\alpha}$  radiation (M18XHF-SRA, MAC Science Co.). In order to obtain enhanced resolution, (111) and (200) reflections were measured by a step scanning with a step size of 0.01° and counting time of 5 s/step.

Electrodes for dielectric measurements with 10 mm diameter were prepared by sputtering platinum. The dielectric constants were measured by using an impedance analyzer (Hewlett Packard, model 4194A, USA) in the frequency range from 100 Hz to 10 MHz at ac electric voltage of 1 V. The samples were placed in a furnace and heated from room temperature to 300 °C during the dielectric measurement. Cooling and heating were performed at a rate of 50 °C/h.

### III. RESULTS AND DISCUSSION

#### A. Stabilization of PZN based solid solutions

Figures 1(a) and 1(b) show x-ray diffraction (XRD) results of 80% PZN+10% PT+10% RN ( $R=K, Na$ ) after calcinations as a function of temperature and PbO excess. The amount of perovskite increased with increasing temperature and the addition of 10% RN accelerated the formation of the perovskite phase. However, the small amount of the pyro-

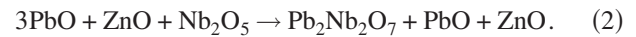
TABLE I. The tolerance factor and electronegativity difference of  $Pb(Zn_{1/3}Nb_{2/3})O_3$ ,  $KNbO_3$ , and  $NaNbO_3$ .

	$Pb(Zn_{1/3}Nb_{2/3})O_3$	$KNbO_3$	$NaNbO_3$
Tolerance factor	0.986	1.054	0.967
Electronegativity difference	1.80	2.23	2.18

chlore phase<sup>23</sup> was still observed even after 1100 °C calcination. In Fig. 1(c), the ratio of a perovskite phase compound was calculated by the following equation:

$$\text{Ratio of perovskite phase (\%)} = \frac{I_{\text{perov}}}{I_{\text{perov}} + I_{\text{pyro}}} \times 100 \quad (1)$$

[ $I_{\text{perov}}$ , intensity of perovskite (110) peak;  $I_{\text{pyro}}$ , intensity of pyrochlore (222) peak]. In 90%PZN-10%PT, the amount of the perovskite phase was smaller than 20% and most of the calcined powders have the pyrochlore phase, as shown in the following equation:<sup>13</sup>



However, when 10% RN was added, the ratio of the perovskite phase increased up to 92%–95% as the calcined temperature increased up to 1000 °C. Above 1000 °C, the ratio of the perovskite phase decreased due to the volatilization of PbO. To compensate the volatilized PbO, 6% of excessive PbO was added to PZN-PT-RN. Figures 1(c) and 1(d) show

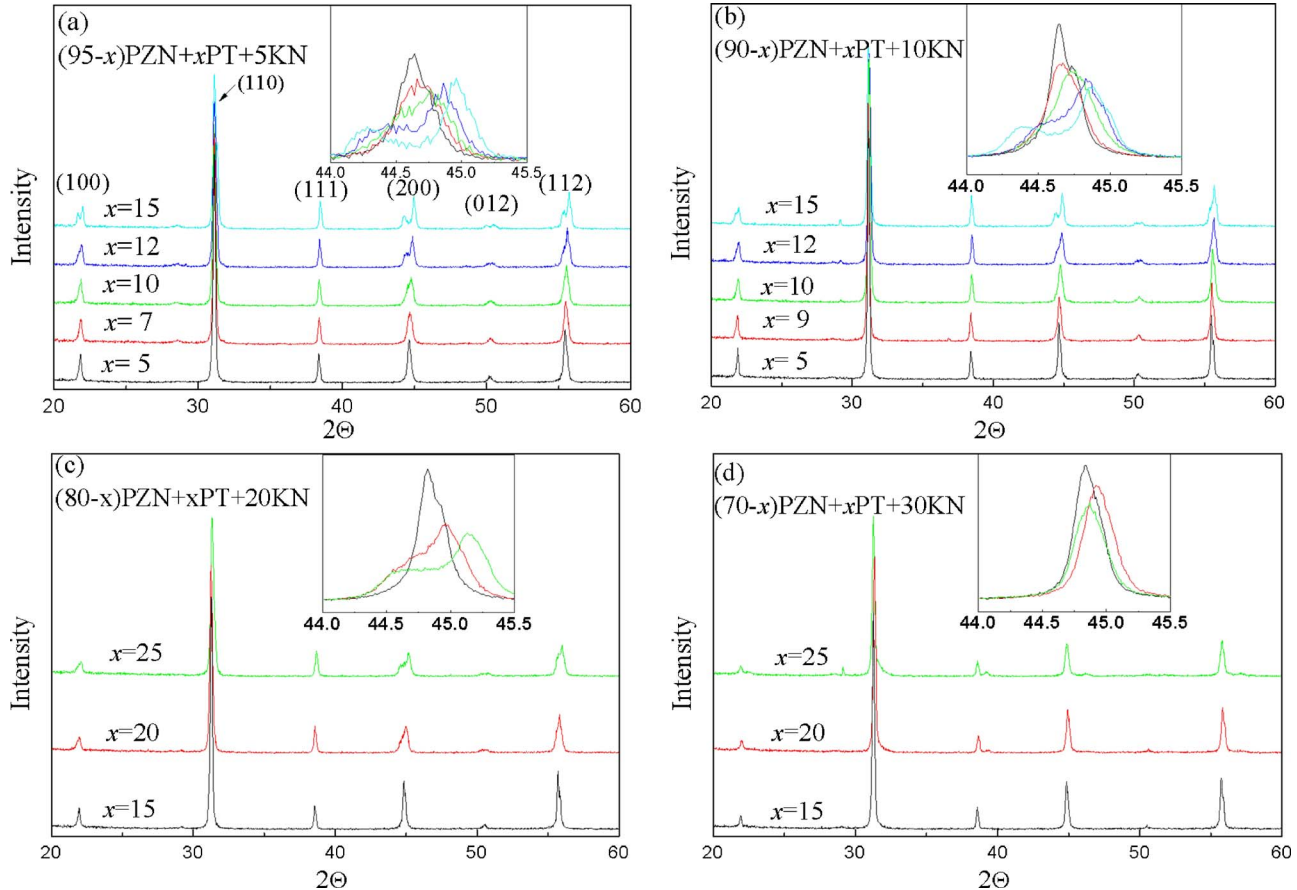


FIG. 2. (Color online) XRD results as a function of the PT( $x$ ) content and the KN( $y$ ) content after calcination at 850 °C and sintering at 1100 °C [compositions=(100- $x$ - $y$ )PZN+ $x$ PT+ $y$ KN+6 mol % Pb excess]; (a)  $y=5$ , (b)  $y=10$ , (c)  $y=20$ , and (d)  $y=30$ .



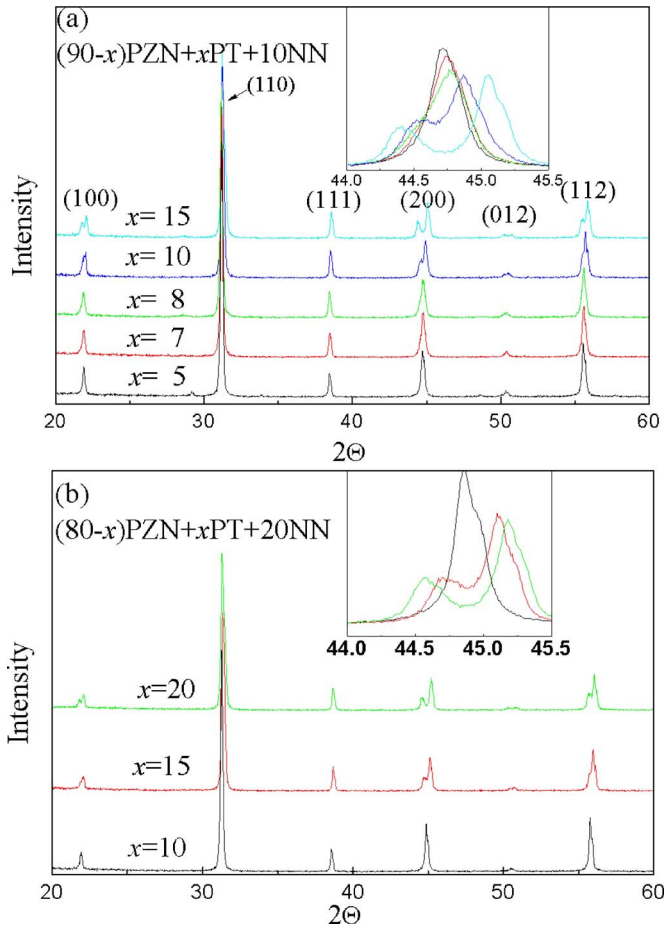


FIG. 3. (Color online) XRD results of as a function of the PT( $x$ ) content and the NN( $y$ ) content after calcination at 850 °C and sintering at 1100 °C [compositions=(100- $x$ - $y$ )PZN+ $x$ PT+ $y$ NN+6 mol % Pb excess]; (a)  $y$  = 10 and (b)  $y$  = 20.

the effect of excess PbO on the phase stability of PZN-PT-RN. Pure perovskite phase was obtained at 1000 °C calcination and maintained at temperature higher than 1000 °C by adding both 10% RN and 6% of excess PbO. Also, it is noted that KN stabilized the perovskite phase more effectively than NN.

There are several possible mechanisms for the stabilization of the perovskite phase such as tolerance factor, electronegativity difference, and repulsive interaction between  $(6s)^2$  lone pair of  $\text{Pb}^{2+}$  cation and  $\text{Zn}^{2+}$  cation.<sup>2</sup> When comprising solid solutions with PZN, both KN and NN decrease the repulsive interaction between  $(6s)^2$  lone pairs of  $\text{Pb}^{2+}$  cation and  $\text{Zn}^{2+}$  cation because smaller  $\text{Nb}^{5+}$  cation is substituted for larger  $\text{Zn}^{2+}$ .<sup>2</sup> The other two factors affecting the stability of the perovskite structure are tolerance factor and electronegativity. The tolerance factor and the electronegativity difference are given by the following equations:

$$t = \frac{\sqrt{2}(r_A + r_O)}{2(r_B + r_O)} \quad (\text{tolerance factor}), \quad (3)$$

$$\chi = \frac{(\chi_{A-O} + \chi_{B-O})}{2} \quad (\text{electronegativity difference}). \quad (4)$$

The tolerance factor and electronegativity difference between cation and anion for PZN, KN, and NN are summarized in

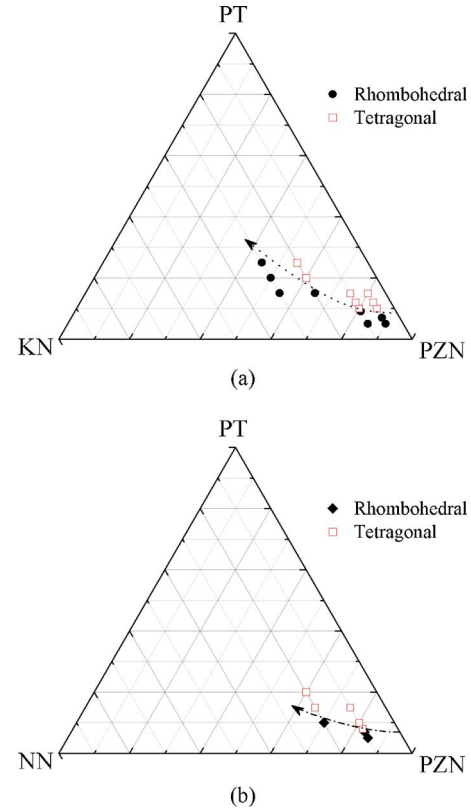


FIG. 4. (Color online) The phase diagram of the PZN-PT-RN ternary system (6 mol % Pb excess); (a) PZN-PT-KN and (b) PZN-PT-NN.

Table I.<sup>2,14</sup> The tolerance factor and electronegativity difference of KN are larger than those of PZN. Therefore, the addition of KN into PZN can increase the tolerance factor and electronegativity difference of PZN based solid solutions. In the case of NN, its tolerance factor is smaller than that of PZN and only its electronegativity difference is larger than that of PZN. Therefore, NN decreases the tolerance factor while it increases the electronegativity difference. It is noted that PZN can be stabilized only by the increase of electronegativity difference though the tolerance factor decreases by adding NN to PZN-PT. This indicates that the electronegativity may be more important to stabilize the perovskite structure of PZN than the tolerance factor. It is shown that three factors contribute to the stabilization of the perovskite phase when KN is added, increased tolerance factor, enhanced electronegativity difference, and decreased repulsive interaction. In the case of addition of NN, the two latter terms contributed to the stabilization of the perovskite structure. This is the reason why KN stabilized the perovskite phase of PZN based solid solutions more effectively than NN.

## B. Change in the MPB of the ternary systems

Figure 2 shows the XRD results of perovskite PZN-PT-KN with 6 mol % Pb excess that are sintered at 1100 °C for 2 h. The inset in Fig. 2 enlarges the (002) peak. The split of peak to (200) and (002) was found with increasing PT content. This indicates the morphotropic phase transition between the rhombohedral and tetragonal phases in the PZN-PT-KN solid solutions. The amount of PT corresponding to

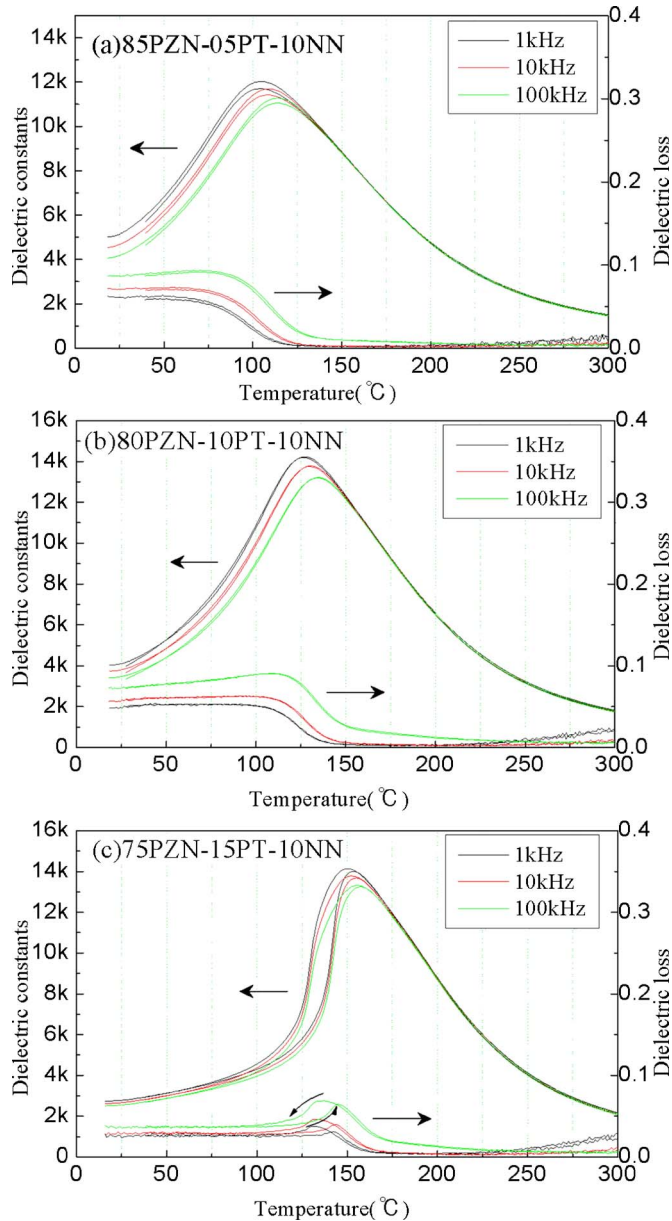


FIG. 5. (Color online) Dielectric properties vs temperature of  $(90-x)\text{PZN}+x\text{PT}+10\text{NN}$ ; (a)  $x=5$ , (b)  $x=10$ , and (c)  $x=15$ .

the MPB of the PZN-PT-KN solid solutions depends on the ratio of KN. As the ratio of KN increases, the MPB range moves to the regime with larger amount of PT.

Figure 3 is the XRD results of the PZN-PT-NN solid solutions with 6 mol % Pb excess that are sintered at 1100 °C for 2 h. The morphotropic phase transition between the rhombohedral and tetragonal phases was observed when 7%–8% PT was added to the solid solution containing 10% NN and 10–15 mol % PT was added to the solid solution containing 20% NN. This also shows that the MPB moved to the regime with larger amount of PT as the amount of alkali niobate increases. In contrast to PZN-PT-KN, the pure perovskite phase of PZN-PT-NN was not synthesized when the amount of alkali niobate was as small as 5 mol %, which can be explained by the different tolerance factors.

Figure 4 shows phase diagrams summarizing the results of XRD analysis on the phase evolution. The amount of PT to induce the morphotropic phase transition ( $x_{\text{PT}}^{\text{MPB}}$ ) is larger

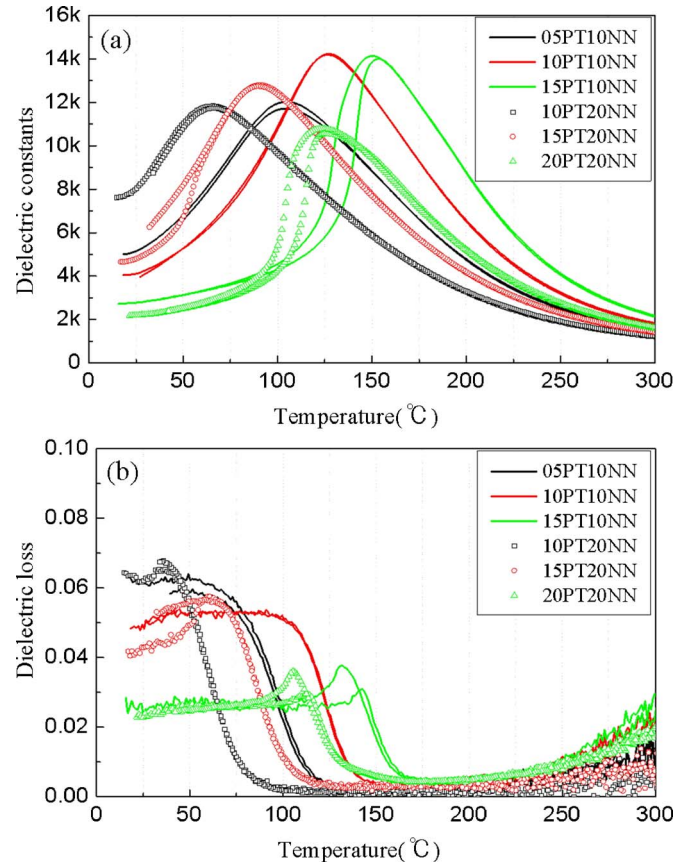


FIG. 6. (Color online) Dielectric properties vs temperature of  $(100-x-y)\text{PZN}+x\text{PT}+y\text{NN}$  at 1 kHz; (a) dielectric constants and (b) dielectric loss.

for PZN-PT-KN than for PZN-PT-NN when the amount of KN is the same as that of NN. This difference in the crystal structure of the solid solution is attributed to the ionic size. When larger K cation (1.64 Å) replaced smaller Pb cation (1.49 Å),<sup>14</sup> the displacement of Pb cation along the [001] direction becomes more difficult due to elastic and electric interactions, and the MPB of the solid solutions was observed in the regime with larger content of PT.<sup>5,15</sup>

### C. Dependence of dielectric properties on temperature

Figure 5 shows dielectric constant versus temperature of PZN-PT-NN. It demonstrates the typical characteristics of relaxor ferroelectrics including the diffuse phase transition (DPT) and the measuring frequency dependence of the temperature of maximum dielectric constant ( $T_{\text{max}}$ ).<sup>16</sup> As the PT content increases, the relaxor behavior weakens and the thermal hysteresis becomes clear [Fig. 5(c)]. These observations indicate that the addition of PT strengthened the first order transition behavior. Figure 6 shows the dielectric constant versus temperature at 1 kHz with 10% and 20% of NN. As shown in Fig. 6,  $T_{\text{max}}$  increased with increasing the PT content and decreasing the NN content. The dielectric constant at  $T_{\text{max}}$  was the highest in the MPB region, so maximum dielectric constants were observed in the 80PZN-10PT-10NN and 65PZN-15PT-20NN. Figure 7 shows dielectric constant versus temperature of PZN-PT-KN. The characteristics of the dielectric constant versus temperature of PZN-PT-KN were similar to those of PZNT-NN system.  $T_{\text{max}}$  decreased with

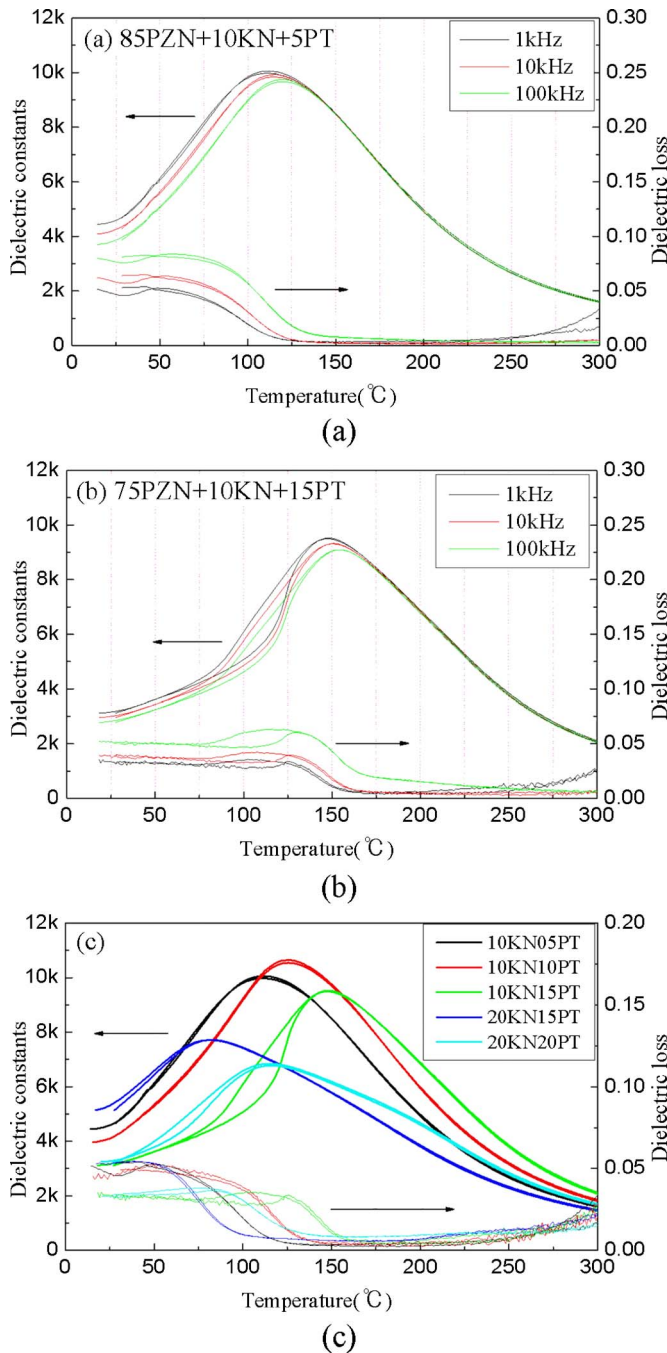


FIG. 7. (Color online) Dielectric properties vs temperature for  $(100-x-y)\text{PZN}+x\text{PT}+y\text{KN}$ ; (a)  $x=5$ ,  $y=10$ , (b)  $x=15$ ,  $y=10$ , and (c) measured at 1 kHz.

decreasing the PT content or increasing the KN content, and the dielectric constant at  $T_{\max}$  was maximized in the MPB region.

The DPT of PZN-PT-RN is analyzed quantitatively by using a diffuseness parameter which Smolenskii and Rolov introduced to express the standard deviation in the Gaussian distribution of Curie temperatures ( $T_C$ ) of individual nanodomains,<sup>17-19</sup>

$$\frac{\epsilon_{\max}}{\epsilon} = 1 + \frac{(T - T_m)^2}{2\delta_g^2}. \quad (5)$$

When  $T \gg T_{\max}$ ,  $\epsilon_{\max}/\epsilon$  is linearly proportional to  $(T - T_m)^2$  and the diffuseness  $\delta_g$  is determined from the slope of  $\epsilon_{\max}/\epsilon$

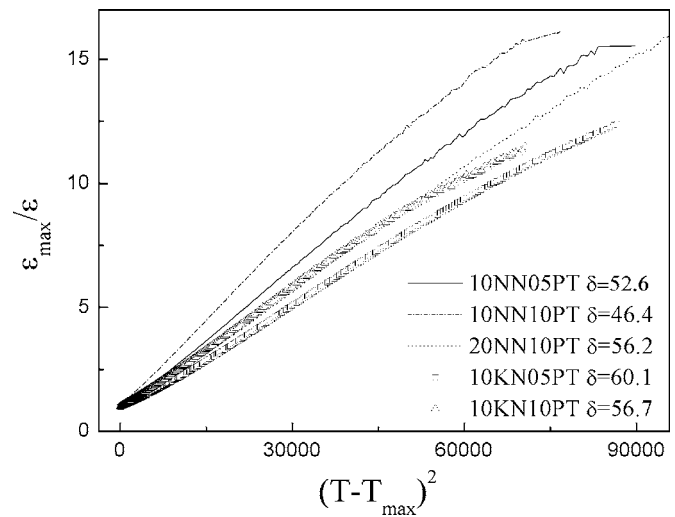


FIG. 8. Diffuseness parameter of  $(100-x-y)\text{PZN}+x\text{PT}+y\text{RN}$ .

vs  $(T - T_m)^2$ . The diffuseness parameter is calculated in Fig. 8. The diffuseness of DPT decreased as the PT content increased or the NN content decreased. In addition, Fig. 8 shows that the diffuseness of PZN-PT-KN is larger than that of PZN-PT-NN. 75PZN-10NN-15PT has a very small  $\delta$  of 44.1, which is consistent with the appearance of the first order phase transition in Fig. 5(c). This indicates that the chemical properties of an individual nanorelaxor including  $T_C$  are more uniform in PZN-PT-NN solid solutions than in PZN-PT-KN.

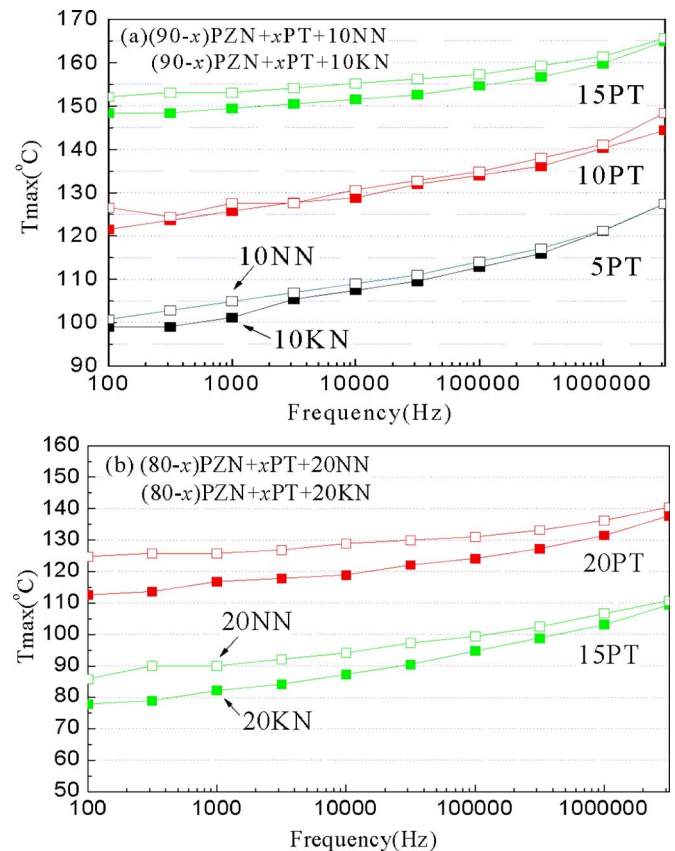


FIG. 9. (Color online)  $T_{\max}$  vs frequency of PZNT-RN ( $R=\text{Li,Na,K}$ ) [composition= $(100-x-y)\text{PZN}+x\text{PT}+y\text{RN}$ ]; (a) 10NN and 10KN and (b) 20NN and 20KN.



In Fig. 9, the temperature for the maximum dielectric constant ( $T_{\max}$ ) of several compositions is summarized as a function of measuring frequency. As shown in Fig. 9, the  $T_{\max}$  of 85PZN-5PT-10RN (100–105 °C) was higher than that of 85PZN-5PT-10BT (53 °C).<sup>4</sup>  $T_{\max}$  increased and the dielectric dispersion with the measuring frequency decreased with increasing the PT content. These observations were more pronounced in PZN-PT-NN, which can be explained as following. When the PT makes the solid solution, the lower tolerance factor of the counterpart material increases the  $T_{\max}$  at the MPB.<sup>5,20</sup> Combined experiments with the first principle calculations on Pb based solid solutions have shown that  $T_{\max}$  is proportional to the square of Pb and B-cation displacement since coupling between nearest-neighboring ferroelectrically active cations increases.<sup>21,22</sup> Small tolerance values indicate that the cations partially fill an A site and there is an empty space in the A site, as shown in Eq. (1). This empty space allows A-site cations to rattle and increases A-site ion displacements. Since a phase transition temperature is proportional to the square of ionic displacements, a small tolerance factor of A-site cation leads to a higher transition temperature by increasing the rattling space of the cations.

#### IV. CONCLUSIONS

We investigated the effect of the tolerance factor and A-site ionic size on the structural and dielectric properties of PZN based solid solutions. The addition of KN and NN to PZN stabilized the perovskite structure effectively. Three stabilization mechanisms contributed to the appearance of the perovskite structure, increased tolerance factor, large electronegativity difference between cation and anion, and decreased repulsion between A-site and B-site cations. KN was found to stabilize the perovskite structure more effectively than NN. However, it is noted that NN can stabilize PZN with the perovskite structure in spite of a smaller tolerance factor. In addition, the phase transition and dielectric properties of PZN-PT-KN and PZN-PT-NN solid solutions were systematically studied. The  $T_{\max}$  of PZN-PT-KN or PZN-

PT-NN was higher than that of PZN-PT-BT and PZN-PT-ST. A comparison of PZN-PT-KN and PZN-PT-NN shows that the  $T_{\max}$  of PZN-PT-NN was higher than that of PZN-PT-KN. We attribute this difference to the smaller tolerance factor of NN which provides larger rattling space to PZN-PT-NN.

<sup>1</sup>S.-E. Park and T. R. Shrout, J. Appl. Phys. **82**, 1804 (1997).

<sup>2</sup>N. Wakiya, N. Ishizawa, K. Shinozaki, and N. Mizutani, Mater. Res. Bull. **30**, 1121 (1995).

<sup>3</sup>L. Bellaiche, J. Padilla, and D. Vanderbilt, Phys. Rev. B **59**, 1834 (1999).

<sup>4</sup>R. E. Eitel, C. A. Randall, T. R. Shrout, and P. W. Rehrig, Jpn. J. Appl. Phys., Part 1 **40**, 5999 (2001).

<sup>5</sup>I. Grinberg, M. R. Suchomel, P. K. Davies, and A. M. Rappe, J. Appl. Phys. **98**, 094111 (2005).

<sup>6</sup>H. Fan, L. Kong, L. Zhang, and X. Yao, J. Appl. Phys. **83**, 1625 (1998).

<sup>7</sup>J. R. Belsick, A. Halliyal, U. Kumar, and R. E. Newnham, Am. Ceram. Soc. Bull. **66**, 664 (1987).

<sup>8</sup>S. Lanfredi, L. Dessemond, and A. C. Martins Rodrigues, J. Eur. Ceram. Soc. **20**, 983 (2000).

<sup>9</sup>B. Jaffe, W. R. Cook, and H. Jaffe, *Piezoelectric Ceramic* (Academic, London, 1971), p. 186.

<sup>10</sup>Y. Xu, *Ferroelectric Materials and Their Applications* (University of California, Los Angeles, 1991), p. 136.

<sup>11</sup>M. Takahashi, Jpn. J. Appl. Phys. **9**, 1236, (1970).

<sup>12</sup>F. Kojima and S. Nomura, Jpn. J. Appl. Phys. **14**, 1255 (1975).

<sup>13</sup>S. Nomura and H. Arima, Jpn. J. Appl. Phys. **11**, 358 (1972).

<sup>14</sup>R. D. Shannon, Acta Crystallogr., Sect. A: Cryst. Phys., Diff., Theor. Gen. Crystallogr. **32**, 751 (1976).

<sup>15</sup>W. Zhu, A. L. Kholkin, P. Q. Mantas, and J. L. Baptista, J. Am. Ceram. Soc. **84**, 1740 (2001).

<sup>16</sup>J. Chen, H. M. Chan, and M. P. Harmer, J. Am. Ceram. Soc. **72**, 593 (1989).

<sup>17</sup>A. A. Bokov and Z.-G. Ye, Solid State Commun. **116**, 105 (2000).

<sup>18</sup>S. M. Pilgrim, A. E. Sutherland, and S. R. Winzer, J. Am. Ceram. Soc. **73**, 3122 (1990).

<sup>19</sup>K. Uchino, S. Nomura, L. E. Cross, S. J. Jang, and R. E. Newnham, J. Appl. Phys. **51**, 1142 (1980).

<sup>20</sup>R. E. Eitel, C. A. Randall, T. R. Shrout, and P. W. Rehrig, Jpn. J. Appl. Phys., Part 1 **40**, 5999 (2001).

<sup>21</sup>J. Grinberg, V. R. Cooper, and A. M. Pappe, Phys. Rev. B **70**, 220101 (2004).

<sup>22</sup>P. Juhas, I. Grinberg, A. M. Rappe, W. Dmonwski, T. Egami, and P. K. Davies, Phys. Rev. B **69**, 214101 (2004).

<sup>23</sup>JCPDS (Joint Committee on Power Diffraction Standards), No. 34-0374 (2000).